MISSION PLANNING UNDER UNCERTAINTY FOR A REUSABLE LAUNCH VEHICLE

Yasmina Bestaoui
Laboratoire IBISC CNRS FRE 3190, Université d'EVRY, FRANCE

Abstract: The first or second stage of a generic Reusable Launch Vehicles (RLV) is in fact constituted by an autonomous airplane that will return to its launching site. The subject of this paper is mission planning under uncertainty. In the beginning, a simple path planning method is introduced using the Frenet-Serret coordinate system then the uncertainty is taken into account by periodic actualizations of the reference paths. Smoothness of paths is an essential feature of navigation of autonomous vehicles.

I. INTRODUCTION

Reusable Launch Vehicles are being pursued as low-cost alternatives to expendable launch vehicles and the shuttle. Two different types of partially reusable launch vehicles are proposed:

- ✓ As a subscale technology demonstrator for a quick turnaround RLV, the X33 (NASA) is an autonomous hypersonic vehicle. The vehicle takes off vertically like a rocket and lands horizontally like an airplane. The unpiloted vehicle has a flight envelope that spans up to 30 miles in altitude and Mach 9 in speeds. On the other hand, ARES-H (ESA) is a winged vehicle which is considered as a typical configuration of the second stage of a reusable vehicle [12, 17].
- ✓ Two stage to orbit system is a promising system as a RLV. This system uses two vehicles: the first one is a winged launcher which accelerates to supersonic region in the atmosphere, the second one is the orbiter. In the beginning of the mission, the winged launcher carrying the orbiter gains altitude and accelerates in the atmosphere and then they separate. The orbiter continues accelerating by itself and finally makes it into space. The winged launcher returns to the launch site after the separation [19].

An airplane is involved in both configurations. Generally, an RLV mission is composed of four major flight phases: ascent, re-entry, Terminal Area Energy Management (TAEM) and Approach & Landing (A&L). RLV in ascent mode involves motion through a wide range of flight condition, wind disturbances and plant uncertainties. Re-entry refers to the movement of the vehicle as it enters the Earth atmosphere from outer space. A&L is a critical flight phase that brings the unpowered vehicle from the end of the TAEM phase to runway touchdown.

Recent advances in guidance technologies have enabled some autonomous aerial vehicle to execute simple mission tasks without human interaction. Many of these tasks are pre-planned using reconnaissance or environment information. The actual trend is towards more autonomy. Task planning and safe trajectory solutions are essential to the survivability and success of an autonomous system. The best path planners adequately trade between accuracy and computation. Because path planning solves for a trajectory over a longer time horizon as compared to the short time horizon of low level control, a considerable advantage can be found if path planning can be done relatively fast. A flight planning algorithm that is robust to changing flight conditions, disturbances and vehicle uncertainties would be an improvement over current RLV flight technology.

One of the most challenging applications is planning under uncertainty. Uncertainty quantification is the process of determining the effect of input uncertainties on response metrics of interest. These input uncertainties may be characterized as either aleatory uncertainties which are irreducible variabilities inherent in nature or epistemic uncertainties which are reducible uncertainties. Probabilistic methods are commonly used for computing response distribution statistics based on input probability distribution specifications. Conversely, for epistemic uncertainties, data is generally sparse, making the use of probability distributions assertions questionable and typically leading to non probabilistic methods based on interval specifications. The major sources of uncertainty are generally classified into three types:

- ✓ stochastic variability: this corresponds to uncertainty arising due to fluctuations that exist in the physical environment (ex; atmospheric conditions)
- ✓ structural uncertainty: any uncertainty arising due to inherent nature of the physical model , assumptions involved, boundary conditions and the numerical discretization.
- ✓ Parametric uncertainty: the uncertainty in the input parameters arising due to the nature of experimental measurements or theoretical calculations (limitations) affects the end result.

The originality of the present paper is the generation of possible **3D** flight paths for an aerial vehicle when maneuvers can also be considered. This paper consists of 6 sections. Section 2 introduces the aircraft translational dynamics. Section 3 presents parametric curves when curvature and torsion are function of the curvilinear abscissa. Section 4 introduces the proposed solution to the uncertainty. Finally, conclusions and perspectives are the subject of Section 5.

II. AIRCRAFT TRANSLATIONAL DYNAMICS

Traditional launch vehicle guidance has employed open loop guidance in the atmospheric phase and closed loop guidance once the vehicle is sufficiently outside the atmosphere. The primary reason is that exo-atmospheric formulations of the guidance problem typically have analytic or near analytic solutions. Though the guidance approaches for the exo-atmospheric phases are efficient and reliable, the use of open loop guidance of the atmospheric flight phase has been one cause of costly launch delays. This occurs when the actual wind profile differs significantly from the mean profile used in computing the attitude control program. The desire to reduce or eliminate this source of launch delay, has led to a renewed interest in developing a closed loop guidance approach for the atmospheric flight phase. The case of 3D flight permits optimization of out-of-plane manoeuvring. In addition, several realistic constraints can be incorporated.

The translational equations of an aerospace vehicle through the atmosphere are directly derived from Newton's law. According to Zipfel [22], if the vehicle flies in the atmosphere with speeds less than Mach 5 (below hypersonic velocity), the Earth can be presumed an inertial reference frame. The aircraft equations of motion are expressed in a velocity coordinate frame attached to the aircraft, considering the velocity of the wind $W = \begin{pmatrix} W_x & W_y & W_z \end{pmatrix}^T$ (components of the wind velocity in the inertial frame). The kinematic equations of the aircraft are given by:

$$\dot{x} = V \cos\chi \cos\gamma + W_x$$
$$\dot{y} = V \sin\chi \cos\gamma + W_y$$
$$\dot{z} = V \sin\gamma + W_z \qquad \text{eq 1}$$

The powered dynamic model used for flight over a flat Earth is the following

$$\dot{V} = -\frac{C_D(M,\alpha)A_{ref}\rho V^2}{2m} - g\sin\gamma + \frac{T\cos\alpha}{m} - \dot{W}_x\cos\gamma\cos\chi - \dot{W}_y\cos\gamma\sin\chi - \dot{W}_z\sin\gamma$$

$$\dot{\gamma} = \frac{C_L(M,\alpha)A_{ref}\rho V\cos\sigma}{2m} - \frac{g\cos\gamma}{V} + \frac{T\sin\alpha\cos\sigma}{mV} + \frac{\dot{W}_x\sin\gamma\cos\chi}{V} - \frac{\dot{W}_y\sin\gamma\sin\chi}{V} - \frac{\dot{W}_z\cos\gamma}{V}$$

$$\dot{\chi} = \frac{C_L(M,\alpha)A_{ref}\rho V\sin\sigma}{2m} + \frac{T\sin\alpha\sin\sigma}{mV\cos\gamma} + \frac{\dot{W}_x\sin\chi}{V\cos\gamma} - \frac{\dot{W}_y\cos\chi}{V\cos\gamma}$$

eq 2

Where x (downrange), y (cross range) and z (altitude) are the vehicle's position, γ is the flight path angle, χ is the azimuth (heading) angle, σ is the bank angle, V is the velocity magnitude, ρ is the free stream mass density, m is the aircraft mass, A_{ref} is a characteristic area for the body, C_L, C_D are respectively the lift and drag coefficient functions that depend upon the Mach number M and angle of attack α. The aircraft flight path angle is the angle γ measured from the horizontal plane to the aircraft's velocity vector in inertial coordinates; the aerodynamic angle of attack α is measured from the aircraft x-y plane to the relative wind velocity vector. The aircraft pitch angle is the angle measured from the inertial horizontal plane to the aircraft x axis. The following relation $\theta = \alpha + \gamma$ is verified. In this kind of applications, the airplane sideslip angle is usually held near zero. The dynamic pressure is $\bar{q} = 0.5\rho V^2$ where the air density ρ at altitude h is approximated using an exponential model $\rho = \rho_0 e^{-\beta h}$ where ρ_0 is the air density at sea level and β is the atmospheric density scale. Generally the lift coefficient is a linear function of the angle of attack $C_L(M) = C_{L_0}(M) + C_{L_\alpha}(M)\alpha$ and the drag coefficient is a quadratic function of C_L :

$$C_D(M) = C_{D_0}(M) + KC_L^2(M) = k_{D_0}(M) + k_{D_1}(M)\alpha + k_{D_2}(M)\alpha^2$$

where C_{D_0} is the drag coefficient at zero lift, K is a coefficient relative to induced drag, $k_{D_O}, k_{D_1}, k_{D_2}$ are resulting coefficients with respect to α .

These equations are called pseudo 5 degrees of freedom. They have an important place in aerospace vehicle study because they can be assembled from trimmed aerodynamic data and simple autopilot designs. Nevertheless, they give a realistic picture of the translational and rotational dynamics unless large angles and cross coupling effects dominate the simulations.

For motion planning purpose, the inverse problem has to be solved. We can thus deduce the velocity

$$V^2 = (\dot{x} - W_x)^2 + (\dot{y} - W_y)^2 + (\dot{z} - W_z)^2$$

eq 3

and the thrust using these relations:

$$T^2 = u_1^2 + u_2^2 + u_3^2$$

eq 4

where

$$u_1 = m\dot{V} + \frac{1}{2}C_D\left(M,\alpha\right)A_{ref}\rho V^2 + mg\sin\gamma + m\dot{W}_x\cos\gamma\cos\chi + m\dot{W}_y\cos\gamma\sin\chi + m\dot{W}_z\sin\gamma$$

$$u_2 = mV\dot{\gamma} - \frac{1}{2}C_L\left(M,\alpha\right)A_{ref}\rho V^2\cos\sigma + mg\cos\gamma - m\dot{W}_x\sin\gamma\cos\chi + m\dot{W}_y\sin\gamma\sin\chi + m\dot{W}_z\cos\gamma$$

$$u_3 = mV\cos\gamma\dot{\chi} - \frac{1}{2}C_L\left(M,\alpha\right)A_{ref}\rho V^2\sin\sigma - m\dot{W}_x\sin\chi - m\dot{W}_y\cos\chi$$

eq 5

Trajectory studies, performance investigations, navigation, guidance evaluations can be successfully executed with simulations of these equations.

III. PARAMETRIC CURVES

A mission describes the operation of an aircraft in a given region, during a certain period of time while pursuing a specific objective. A flight plan is defined as the ordered set of movements executed by the aircraft during a mission. It can be decomposed in phases. Each phase is described by the coordinates of a pair of way-points and by the speed at which the aircraft is to fly between these way-points. A phase is completed when the second way-point is reached by the aircraft. Path planning in an autonomous vehicle provides the level of autonomy by having minimal ground control. Classically, in motion planning and generation, methods such as continuous optimization and discrete search are sought. Lavalle [15] presented a randomized motion planning algorithm by employing obstacle free guidance system as local planners in a probabilistic roadmap framework. Yakimenko [20] based path planning of autonomous fixed wing aircraft on a learning real-time A* search algorithm, considering only the motion on a horizontal plane. A family of trim trajectories in level flight is used in all these references to construct paths. Frazzoli et al [11] described motion plans as the concatenation of a number of well defined motion primitives selected from a finite library. They use a ‘maneuver automaton, defining rules for the concatenation of primitives in the form of a regular language, a maneuver being defined as a non trivial primitive which is compatible from the beginning and the end with trim primitives. Atkins et al [2, 3] introduced the concepts of a parameterized flight plan, a plan with at least one symbolic parameter, and flight plan instantiation, the process by which symbolic parameters in a parameterized flight plan are instantiated to values for which specified requirements are satisfied.

Classical differential geometry curve theory is a study of 3D space curves with orthogonal coordinate systems attached to moving points on the space curve. Trajectory planning is an optimization problem which generates an optimal trajectory between two configurations in the state space, considering a given performance index (time, energy or distance). Its feasibility depends on the choice of the optimization method, the performance index and a number of constraints from various nature, the latter depend essentially on the vehicle itself (architecture, dynamics and actuation modes) and the environment in which the vehicle moves (endurance, airspeed, altitude, landing and takeoff modes ...) [5-6,9,18].

For convenience, time is not chosen to be the independent variable in this paragraph. We are interested by the curvilinear abscissa s instead of the time, let’s consider the curve C(s) representing the motion of this vehicle in $\mathbf{R}^3$, where $V = \frac{ds}{dt}$. The Frenet-Serret coordinate system [4,5,7,8,16] is used to study the shape of a space curve. In 3D space, the following flight path is characterized in steady air:

$$dx = \cos\chi\cos\gamma\, ds$$

$$dy = \sin\chi\cos\gamma\, ds$$

$$dz = \sin\gamma\, ds$$

Two non-holonomic constraints can thus be deduced:

$$dx\sin\chi - dy\cos\chi = 0$$

$$\left[dx\cos\chi + dy\sin\chi\right]\sin\gamma - dz\cos\gamma = 0$$

For non holonomic vehicles such as mobile robots or aerial vehicles, dynamic model and actuators constraints that directly affect path are used to reject infeasible paths. The term feasible means that the path will be continuously flyable and safe. The flyable path should be smooth, i.e. without twists and cusps. The smoothness of the path is determined by amount of bending of the path measured by curvature and torsion of the path. If a non vanishing curvature and a torsion are given as smooth functions of s, theoretically both equations can be integrated to find the numerical values of the corresponding space curve (up to a rigid motion).

The focus is on turning a sequence of configurations into a smooth curve that is then passed to the control system of the vehicle. The curves used fall into two categories:

- ✓ curves whose coordinates have a closed form expression for example B-splines, quintic polynomials or polar splines [14, 16]
- ✓ parametric curves whose curvature is a function of their arc length for example clothoids, cubic spirals, quintic G^2 splines or intrinsic splines [4, 5,10, 11, 13, 18].

However, significant research efforts are still needed to advance the state of the art of trajectory planning for autonomous aerospace vehicles. In the previous papers, the proposed trajectories are based on classical trim helices and non equilibrium trajectories are not considered. In these papers, the atmosphere was considered to be an isotropic and homogeneous medium, i.e. when there is no wind and the air density is constant with altitude. Jiang and Ordonez [12] proposed 2D maneuvers in the vertical flight for the approach and landing for unpowered reusable launch vehicle while Shanmugavel et al [18] are using the well-known clothoid arcs to join trim paths at constant altitude.

The shape of a space curve can be completely captured by its curvature and torsion. Using the Frenet-Serret formulation, curvature χ as well as torsion τ can be deduced (‘represents the derivation versus s):

$$\kappa(s) = \frac{\|C' \times C''\|}{\|C'\|^3} = \sqrt{\gamma'^2 + \chi'^2\cos^2\gamma(s)}$$

$$\tau(s) = \frac{\chi'\gamma''\cos\gamma + 2\chi'\gamma'^2\sin\gamma - \gamma'\chi''\cos\gamma - \gamma'\chi'^2\cos\chi\cos\gamma\sin\chi\sin^2\gamma + \chi'^3\cos^2\gamma\sin\gamma}{\gamma'^2 + \chi'^2\cos^2\gamma}$$

The purpose of this paragraph is to propose a 3D flight path to the aerial vehicle joining two consecutive waypoints configurations. The inputs of this path planning algorithm are the i[th] way-point configuration parameters $x_i, y_i, z_i, \chi_i, \gamma_i$ and the (i+1)th configuration parameters: $x_{i+1}, y_{i+1}, z_{i+1}, \chi_{i+1}, \gamma_{i+1}$. Depending on these parameters, many possibilities exist. The most obvious one would be to propose a polynomial variation of x, y and z. However the main drawback is a complicated formulation of the curvature and the torsion making control of smoothness (twists and cusps) a difficult task. The approach followed in this paper aims to propose a simple formulation of these two parameters.

3.1 Constant curvature and torsion

The heading and flight path angles can be given by the following relations

$$\chi(s) = \chi_0 + s\chi_1 \qquad \gamma(s) = \gamma_i$$

While the curvilinear abscissa is given simply by a linear temporal relation as the velocity is constant.

$s = V_i t \qquad\qquad 0 \le t \le \tau$

with the constant curvature and torsion $\kappa(s) = \chi_1 \cos(\gamma_0) \qquad\qquad \tau(s) = \chi_1 \sin(\gamma_0)$

Figure 1 shows the obtained path obtained after integration of eq. 1, assuming that there is no wind.

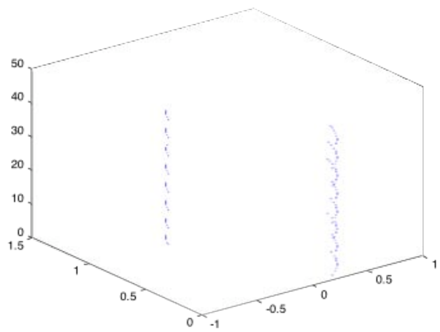

Figure 1: trim helicoidal path (units in 1000m)

Cylindrical helices are classically known in aeronautical science to be trim conditions. A trimmed flight condition is defined as one in which the rate of change of magnitude of the aerial vehicle state vector is zero (in the body fixed frame) and the resultant of the applied forces and moments are zero. The following non linear equations system has to be solved in order to determine the reference thrust and attack and bank angles.

$$0 = -C_D(M,\alpha)A_{ref}\rho V^2 - 2mg\sin\gamma + 2T\cos\alpha$$

$$0 = C_L(M,\alpha)A_{ref}\rho V\cos\sigma V - 2mg\cos\gamma + 2T\sin\alpha\cos\sigma$$

$$0 = C_L(M,\alpha)A_{ref}\rho V^2\sin\sigma\cos\gamma + 2T\sin\alpha\sin\sigma$$

In a trimmed maneuver, the aerial vehicle will be accelerated under the action of non zero resultant aerodynamic and gravitational forces and moments: effects such as centrifugal and gyroscopic inertial forces and moments will balance these effects.

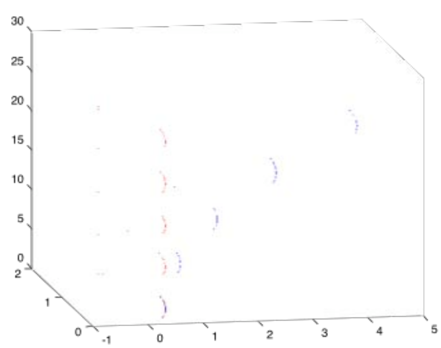

Figure 2: Trim helicoidal motion with (blue) and without (red) steady wind(units in 1000m)

Figure 2 shows the effect of a steady wind on the trim trajectory (in red). The blue curve represents a helix with a translation in the x direction. In 2D plane, a trochoidal curve is obtained. The influence of the curve is bigger as time passes by.

3.2 Linear curvature and torsion

The flight path angle is assumed constant while the heading angle has a quadratic variation versus s.

$$\chi(s) = \chi_0 + s\chi_1 + s^2\chi_2 \qquad \gamma(s) = \gamma_i$$

$$s = \frac{1}{2}\frac{V_{i+1} - V_i}{\tau}t^2 + V_i t \qquad 0 \le t \le \tau$$

with the linear curvature and torsion $\kappa(s) = (\chi_1 + 2\chi_2 s)\cos(\gamma_0) \quad \tau(s) = (\chi_1 + 2\chi_2 s)\sin(\gamma_0)$

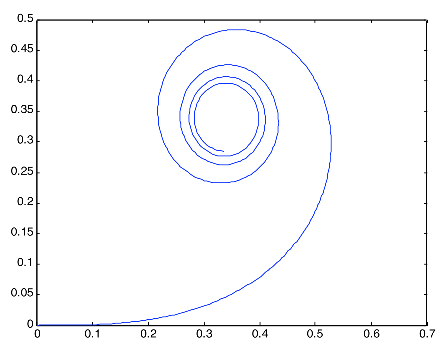

Figure 3: path in the x-y plane without wind
The units are in (1000m).

Figure 3 show the path in the x-y plane corresponding to a clothoid (a well known curve in mobile robotics and highway design) while 3D Path is shown in figure 4 assuming first that there is no wind (red curve) and in second, that the steady wind is in the x direction (blue curve).

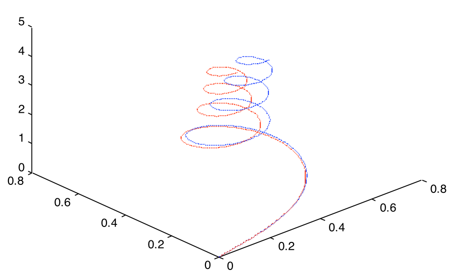

Figure 4: Linear torsion and curvature3D curve with (blue) and without (red) steady wind (units in 1000m)

The reference thrust and bank angle can be determined via the resolution of this system of nonlinear equations.

$$\frac{V_{i+1}-V_i}{\tau}=-\frac{C_D(M,\alpha)A_{ref}\rho V^2}{2m}-g\sin\gamma+\frac{T\cos\alpha}{m}$$
$$0=\frac{C_L(M,\alpha)A_{ref}\rho V\cos\sigma}{2m}-\frac{g\cos\gamma}{V}+\frac{T\sin\alpha\cos\sigma}{mV}$$
$$\frac{\chi_{i+1}-\chi_i}{\tau}=\frac{C_L(M,\alpha)A_{ref}\rho V\sin\sigma}{2m}+\frac{T\sin\alpha\sin\sigma}{mV\cos\gamma}$$

This approach can be easily generalized with a higher order polynomial. If the heading angle is chosen as a cubic polynomial, the obtained curve in the x-y plane, is known as a cubic spiral [13].

3.3. Nonlinear curvature and torsion

In this case, a linear variation of both the heading and flight path angles is assumed:

$$\chi(s)=\chi_0+s\chi_1 \qquad \gamma(s)=\gamma_0+s\gamma_1$$
$$s=\frac{1}{2}\frac{V_{i+1}-V_i}{\tau}t^2+V_it \qquad 0\le t\le\tau$$

with the nonlinear curvature and torsion $\kappa(s)=\sqrt{\gamma_1^2+\chi_1^2\cos(\gamma_0+\gamma_1 s)};\tau(s)=(\chi_1+2\chi_2 s)\sin(\gamma_0)$

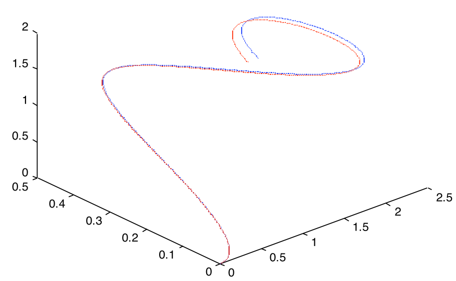

Figure 5: 3D curve with linear varying heading and flight path angles with (red) and without steady wind

A generalization in this sense would give a more complicated formulation of the curvature and the torsion.

3.4. Maneuvers

The problem of maneuvers between two different trim trajectories is an important problem in motion planning for an aerial vehicle. Let's consider the case of joining a trim path to a non trim on as in paragraph 3.2. in the case of a constant flight angle γ_1. Let L_1 and L_2 be respectively the length of the first and the second part. The coordinates of the junction point (x_j, y_j, z_j, χ_j) have to be determined, by the resolution of a set of nonlinear equations.

$$x_j=x_i-\frac{\cos\gamma_i}{\chi_1}(\sin\chi_j-\sin\chi_0)$$
$$y_j=y_i+\frac{\cos\gamma_i}{\chi_1}(\cos\chi_j-\cos\chi_0)$$
$$z_j=z_i+L_1\sin\gamma_i=z_f-L_2\sin\gamma_i$$

The following simulation results are used to join a trim path (in bold blue) to a non-trim path (in thin green) with constant torsion and linear curvature. The initial configuration for both paths is $x_0 = 0m, y_0 = 0m, z_0 = 100m, \chi_0 = 0rad; \gamma_0 = 0.1rad$. For the trim path, the final configuration is $x_t = 900m, y_t = 1400m, z_t = 300m, \chi_t = 2rad; \gamma_t = 0.1rad$ For the non trim path, the final configuration is $x_{nt} = 400m, y_{nt} = 950m, z_{nt} = 300m, \chi_{nt} = 4rad; \gamma_{nt} = 0.1rad$. Trim and non trim 3D paths are shown in figure 6 (the units are in m).

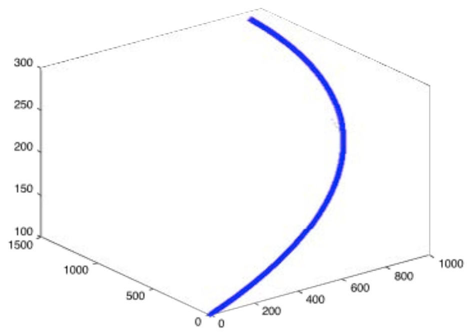

Figure 6: 3D trim (thin line) and non trim (bold line) paths with linear curvature

The role of the trajectory generator is to generate a feasible time trajectory for the aerial vehicle. Once the path has been calculated in the Earth fixed frame, motion must be investigated using the dynamic model and reference trajectories determined taking into account actuators constraints (inequality constraints) and the under-actuation (equality constraints) of an aerial vehicle and limitations on curvature and torsion. Moreover, it is desirable that the plan makes optimal use of the available resources to achieve the goal optimizing some 'cost' measure: the time, energy … required for the execution.

IV. UNCERTAINTY

Path planning involves creating a plan to guide an aerial vehicle from its initial position to a destination way-point. Along the way, there may be a set of regions to visit and a set of regions to avoid. In addition, the traveling object may have certain motion constraints. The path planning strategy could be either static or dynamic depending on whether the path planning problem is to create a path in static or in dynamic environment [17]. Path planning routines will attempt to create paths that are fully consistent with the physical constraints of the aircraft. Path planner takes into account the obstacle avoidance [21], shortest and optimum flight path and weighed regions. Weighed regions are regions with abnormally low or high pressure, wind speeds or any other factor affecting flight.

There is a need for uncertainty model that can mitigate the effect of the lack of fidelity in the analysis. This type of uncertainty that arises due to simplifying the level of fidelity in the analysis is referred to as epistemic uncertainty in the literature. Epistemic uncertainty is defined as a potential deficiency in any phase or activity of the modeling process that is due to lack of knowledge. Fidelity uncertainty means epistemic uncertainty. This type of uncertainty arises when new classes of systems are developed for the first time. In such situations, there is a scarcity of high fidelity information. Probabilistic approaches to handle uncertainty associated with low/medium fidelity analysis can be used; the function can be computationally expensive, restricting its frequent use while searching the design space during optimization. Alternative approaches that are not based on probabilistic theory can also be investigated.

In this paper, the idea is simple: as uncertainty always exists due to numerous reasons, a way of taking care of it is to actualize periodically the reference paths. If due to the wind effect, the aircraft has overshoot the way point it was supposed to go through, then the next way point should be considered. The immediate measurements of the position and orientation are taken as initial conditions for the next reference trajectories. The machinery introduced in Section 3 is used for that purpose.

V. CONCLUSIONS

Path planning is still one of the open problems in the field of autonomous systems. It is a complex problem involving respect of physical constraints on the vehicle, on the environment and other operational requirements. This paper addresses the problem of characterizing continuous paths in 3D. Parametric paths with given curvature and torsion are investigated. Two particular cases are studied: constant, linear and quadratic variation of the heading angle versus the curvilinear abscissa, with the assumption of a constant or linear variation of the flight path angle, to consider different kinds of maneuvers. Depending on the mission, time variable velocity must be considered, giving more flexibility to the trajectory generator, with respect to the limitations on actuators, on curvature and torsion. Issues such as actuator saturation are also being addressed. The proposed solution to uncertainty is a periodic actualization of the reference paths.

References :

[1] Aljarrah M.A., Hasan M.M. (2009) 'HILS setup of dynamic flight path planning in 3D environment with flexible mission planning using ground station' Journal of the Franklin Institute, 2009.02.010

[2] Atkins, E. , Abdelzaher, T.F., Shin. K.G., Durfee E. H. (2001) 'Planning and resource allocation for hard real-time, fault tolerant plan execution' Autonomous agents and multi-agents, vol. 4, pp. 57- 78

[3] Atkins E., Portillo I. A., Strube M. J. (2006)'Emergency flight planning applied to total loss of thrust' Journal of Aircraft, Vol. 43, #4, pp. 1205-1216

[4] Avanzini, G. (2004): Frenet based algorithm for trajectory prediction. AIAA J. of Guidance, Control, Dynamics, vol. 27, 127-135

[5] Bestaoui, Y. (2007): Path Generation for an UAV using the Frenet-Serret frame, AIAA Infotech@aerospace, Rohnert Park, California.

[6] Bestaoui, Y., Dahmani H., Belharet K. (2009a): Geometry of translational trajectories for an autonomous aerospace vehicle with wind effect. 47^{th} AIAA Aerospace Sciences Meeting, Orlando, Florida, paper AIAA-1352.

[7] Bestaoui, Y. (2009b): Geometrical properties of aircraft equilibrium and non equilibrium trajectory arcs, IEEE Workshop on Robot Motion Control, Czerniejwo, Poland.

[8] Bloch, A.M. (2003): Non Holonomics Mechanics and Control. Springer-Verlag, Berlin

[9] Boukraa, D, Bestaoui, Y., Azouz, N. (2008): Three Dimensional Trajectory Generation for an Autonomous Plane. International Review of Aerospace Engineering, Vol. 4, 355-365

[10] Fraichard, T, Scheuer, A(2008): From Reeds and Shepp's to Continuous Curvature Paths. IEEE Transactions on Robotics, Vol. 20, 1025-10355

[11] Frazzoli, E., Dahleh, M.A., Feron, E. (2008): Maneuver Based Motion Planning for Nonlinear Systems with Symmetries. IEEE Transactions on Robotics, Vol. 4, 355-365

[12] Jiang Z., Ordonez R. (2009) 'On-line robust trajectory generation on approach and landing for reusable launch vehicles ' Automatica, 2009.03.017.

[13] Kanayama Y., Fahroo F. (1997): A new line tracking method for non holonomic vehicles. IEEE Int. Conf. On Robotics & Automation, Albuquerque, NM, pp. 2908-2913.

[14] Laumond J.P. ed. (1998) ‘Robot motion planning and control’ New York, Springer, 1998, vol. 229, Lecture Notes in Control and Information Sciences

[15] Lavalle, S.M. (2006): Planning Algorithms. Cambridge University Press

[16] Nelson, R., Barber, B., McLain, T., Beard, R. (2007): Vector Field Path Following for Miniature Air Vehicle, IEEE Transactions on Robotics. Vol. 23, 519—529

[17] Shaffer P., Ross I.M., Oppenheimer M. W., Doman D.B., Bollino K. P. (2007) ‘Fault Tolerant optimal trajectory generation for reusable launch vehicles’ Journal of Guidance, control and dynamics, vol. 30, #6, pp. 1794-1802

[18] Shanmugavel M., Tsourdos A., White B., Zbikowski R. (2009) ‘Co-operative path planning of multiple UAVs using Dubins paths with clothoid arcs ’ Control Engineering Practice, 2009.02.010

[19] T. Uematsu, T. Ishida, S. Aso, Y. Tani (2009) ‘Reduction of aerodynamic interference for separation of two stage reusable launch vehicles’ 47th AIAA Aerospace Sciences Meeting, AIAA 2009-1101

[20]Yakimenko, O.A. (2000): Direct Method for Rapid Prototyping of Near Optimal Aircraft Trajectory. AIAA. Journal of Guidance, Control and Dynamics, Vol. 23, 865--875

[21] H.I. Yang, Y. J. Zhao (2004) ‘Trajectory planning for autonomous aerospace vehicles amid known obstacles and conflicts’ Journal of Guidance, Control & Dynamics, vol. 27, #6, pp. 997-1008

[22] Zipfel P. H. (2007)‘Modeling and simulation of aerospace vehicle dynamics’ AIAA Education Series, 2nd edition, Reston, VA